

Primordial Li Reduction Induced by a Long-lived MeV Sterile Neutrino

Hiroyuki Ishida,^{1,*} Motohiko Kusakabe,^{2,3,†} and Hiroshi Okada^{4,‡}

¹*Department of Physics, Tohoku University, Sendai 980-8578, Japan*

²*School of Liberal Arts and Science, Korea Aerospace University, Goyang 412-791, Korea*

³*Department of Physics, Soongsil University, Seoul 156-743, Korea*

⁴*School of Physics, KIAS, Seoul 130-722, Korea*

We study the feasibility whether or not a sterile neutrino could solve the primordial Li problem within a simple model; that is, standard model plus a sterile neutrino. We analyze effects of the decay of sterile neutrino on cosmological observables, and show that partial reduction can be achieved in the parameter regions of $\mathcal{O}(10)$ MeV for sterile neutrino mass and $\mathcal{O}(10^5)$ sec for its lifetime, which are consistent with both constraints from experiments of the sterile neutrino searches and astrophysical observations. We also show the possibility of detection of the sterile neutrino, measuring the decay such as $\pi^+ \rightarrow \mu^+ + \nu_s$.

I. INTRODUCTION

Big bang nucleosynthesis (BBN) model [1] successfully explains primordial light element abundances inferred from astronomical observations (*e.g.* [2, 3]) if the cosmological baryon density determined from the power spectrum of cosmic microwave background (CMB) radiation measured with the Wilkinson Microwave Anisotropy Probe (WMAP) [4–7] is adopted. An apparent discrepancy, however, exists between observational and theoretical ${}^7\text{Li}$ abundances. Spectroscopic observations of metal-poor stars (MPSs) indicate a plateau for the abundance ratio, ${}^7\text{Li}/\text{H} = (1 - 2) \times 10^{-10}$, with small error bars as a function of metallicity [8–21]. This abundance is smaller by a factor of $\sim 3 - 4$ than that predicted in standard BBN (SBBN) model (*e.g.*, ${}^7\text{Li}/\text{H} = 5.24 \times 10^{-10}$ [2]; see Ref. [3] for theoretical light element abundances for the baryon density from Planck reported in preprint [22]). This Li problem (see Ref. [23] for a review) shows that some physical processes have reduced the primordial Li abundance in some epoch during or after BBN.

Standard stellar model suggests very small depletions of Li isotopes in surfaces of MPSs [24]. The ${}^7\text{Li}/\text{H}$ abundances of MPSs observed today are then approximately interstellar abundances when the MPSs formed. Nonstandard processes such as the rotationally induced mixing [25, 26], and the turbulent mixing [27–29] have been suggested to reduce the ${}^7\text{Li}$ abundance in stellar atmospheres. In the former model, a large depletion factor does not realize simultaneously with a small dispersion in stellar Li abundances after the depletion that observations indicate. The depletion factor is then constrained to be small. In the latter model, a depletion of a factor of $1.6 - 2.0$ [27] is predicted although it is still unclear if this mechanism can deplete Li abundances of all MPSs rather uniformly.

Nonstandard BBN, on the other hand, may be responsible for the Li problem at least partially. We note that ${}^7\text{Be}$ is produced more than ${}^7\text{Li}$ is in SBBN model with the WMAP baryon density. The ${}^7\text{Be}$ nuclei are then converted to ${}^7\text{Li}$ nuclei via recombination with electron followed by the electron capture, *i.e.*, ${}^7\text{Be} + e^- \rightarrow {}^7\text{Li} + \nu_e$. Therefore, the Li problem is alleviated if some exotic processes could destroy ${}^7\text{Be}$. One of solutions to the Li problem is an injection of nonthermal photon with energy of ~ 2 MeV which can destroy ${}^7\text{Be}$ but not Deuterium (D) as calculated in Ref. [30]. If a long-lived exotic particle radiatively decays during or after BBN, nonthermal photons can disintegrate background thermal nuclei, and light element abundances change [31]. If the energy of the photon emitted at the decay is much larger than $\mathcal{O}(10)$ MeV, all of light nuclei are disintegrated by nonthermal photons [31–43]. In this case, therefore, the Li problem can not be solved (*e.g.* [41, 43]). For this reason, the energy of emitted photon for the ${}^7\text{Be}$ destruction is limited to a narrow range. A similar ${}^7\text{Be}$ destruction occurs if a long-lived sterile neutrino decays into energetic electron and positron, so that we study the cosmological effects of the decay.

In the theoretical point of view of the extended Minimal Standard Model (MSM), right-handed neutrinos as sterile neutrinos actually provide an elegant solution to generate tiny active neutrino masses; so-called canonical seesaw mechanism, as well as the origin of the baryon asymmetry of the universe; so-called leptogenesis scenario [44], if their masses are so heavy (more than 10^9 GeV). Even if the sterile neutrinos have masses below electroweak (EW) scale, however, there exist the other phenomenological aspects without lacking the success of the seesaw mechanism. One of

*Electronic address: h-ishida@tuhep.phys.tohoku.ac.jp

†Electronic address: motohiko@kau.ac.kr

‡Electronic address: hokada@kias.re.kr

the biggest issues is detectability of the sterile neutrinos and several possibilities are investigated (for recent study, see [45] and the references therein), and we have especially studied in detail the case, where sterile neutrinos are lighter than relatively light mesons (*e.g.* pion or kaon). The allowed parameter space for the sterile neutrinos masses smaller than the pion mass ~ 140 MeV is not consistent with the recent neutrino oscillation experimental results, unless one assumes that their lifetimes are longer than ~ 0.1 sec. In addition, a constraint has been derived from a study of BBN by a comparison between theoretical and observational abundances of ^4He . The upper limit on the lifetime of ~ 0.1 sec was derived when a relic abundance of sterile neutrino is fixed as given in Ref. [47, 48]. However, this constraint depends on the relic abundance. We then consider the possibility that the abundance is smaller than the simple estimate [47, 48]. In this case a longer lifetime of the sterile neutrino is allowed.

In this paper, we revisit cosmological effects of a long-lived light sterile neutrino. In Sec. II, we assume a decay of a sterile neutrino, and describe a formulation of the nonthermal nucleosynthesis triggered by the decay in the early universe. In Sec. III, we show energy spectra of electron and positron emitted at the decay, energy spectra of energetic photon produced via inverse Compton scattering of background photons by the electron and positron, and photon injection spectra resulting from electromagnetic cascade showers. Abundances of D and ^7Li are then calculated with the nonthermal photons taken into account. In addition, we calculate changes of the baryon-to-photon ratio and the effective neutrino number by the decay. In Sec. IV, we discuss about initial abundance of the sterile neutrino decay and experimental constraints from pion decay measurements. In Sec. V, this study is summarized. In Appendix A, formulae of sterile neutrino decay are described, and in Appendix B, adopted cross sections for photodisintegration of ^7Be and ^7Li are described. We adopt natural units of $\hbar = c = k_B = 1$, where \hbar is the reduced Planck constant, c is the speed of light, and k_B is the Boltzmann constant. We also adopt notation of $A(a, b)B$ for a reaction $A + a \rightarrow b + B$.

II. MODEL

In this paper, we simply introduce one right-handed (sterile) neutrino, N , into the MSM and assume that it has $\mathcal{O}(10)$ MeV mass scale and rather long lifetime $\sim \mathcal{O}(10^5)$ sec. We reconsider effects of the decays of $\mathcal{O}(10)$ MeV sterile neutrino on cosmological quantities, especially the Li abundance, *i.e.*, $^7\text{Li}/\text{H}$.

A. Method

We perform a BBN calculation. Kawano's BBN code [49, 50] is utilized, and Sarkar's correction for ^4He abundances [51] is adopted. Reaction rates for light nuclei ($A \leq 10$) are updated with recommendations by JINA REACLIB Database V1.0 [52]. The neutron lifetime is set to be $878.5 \pm 0.7_{\text{stat}} \pm 0.3_{\text{sys}}$ s [53, 54] based on improved measurements [55].

We adopt cosmological parameters reported from the analysis of the WMAP [4–7]. Central values for model ΛCDM (WMAP only) determined from the latest published WMAP9 data are $H_0 = 70.0 \pm 2.2$ km s $^{-1}$ Mpc $^{-1}$, $\Omega_b = 0.0463 \pm 0.0024$, $\Omega_\Lambda = 0.721 \pm 0.025$, $\Omega_m = 0.279 \pm 0.025$, and $\eta = (6.19 \pm 0.14) \times 10^{-10}$ [7].

It is assumed that energetic electrons and positrons are generated at the decay of a long-lived massive particle (sterile neutrino) N . The sterile neutrino N has a mass M_N and a mean lifetime of τ_N . Through the inverse Compton scattering of cosmic background radiation (CBR), the energetic electrons and positrons produce energetic primary photons. The energy of the photons is related to the energy of e^\pm and temperature of the universe.

The present model has three parameters regarding effects of nonthermal nucleosynthesis: (1) (n_N^0/n_γ^0) is the number ratio of the decaying particle N to the background photon evaluated before the decay of N , (2) τ_N is the lifetime of N , and (3) $E_{N \rightarrow e}$ is the total energy of e^\pm emitted at one N decay event which is equivalent to the energy injected in the form of electromagnetic cascade showers. We adopt the method of Ref. [43] to calculate the nonthermal nucleosynthesis, where thermonuclear reactions are simultaneously solved. We utilized updated reaction rates of ^4He photodisintegration [Eqs. (2) and (3) of Ref. [56]] based on cross section data from measurements with laser-Compton photons [57, 58]. In this work, we found errors in cross sections of reactions $^7\text{Be}(\gamma, \alpha)^3\text{He}$ and $^7\text{Li}(\gamma, \alpha)^3\text{H}$ [39] adopted in previous studies on the BBN model with the decaying N particle. The errors are then corrected in this calculation as explained in Appendix B.

B. injection spectrum of photon

The injection spectrum of nonthermal photon is given by

$$p_\gamma(E_\gamma, T, M_N) = \frac{1}{\Gamma} \int_{m_e}^{M_N/2} \frac{d\Gamma}{dE_e}(M_N) dE_e \int_0^{E_{\gamma 0, \max}} P_{\text{IC}}(E_e, E_{\gamma 0}, T) p_{\gamma, \text{EC}}(E_\gamma, E_{\gamma 0}, T) dE_{\gamma 0}, \quad (\text{II.1})$$

where T is the temperature of the universe, $(1/\Gamma)d\Gamma/dE_e(M_N)$ is the differential decay rate as a function of energy of e^\pm and M_N [cf. Eq. (A.15)], $P_{\text{IC}}(E_e, E_{\gamma 0}, T)$ is the energy spectrum of primary photon ($E_{\gamma 0}$) produced at inverse Compton scatterings by e^\pm with energy E_e at temperature T , and $p_{\gamma, \text{EC}}(E_\gamma, E_{\gamma 0}, T)$ is the energy spectrum of nonthermal photon which is realized after the electromagnetic cascade showers of primary photon of energy $E_{\gamma 0}$ at T .

C. decay of sterile neutrino

The Lagrangian of neutrino sector by adding one Majorana sterile neutrino, N , is given as

$$\mathcal{L} = \bar{N} \gamma_\mu \partial^\mu N - F_\alpha \bar{L}_\alpha H N - \frac{M_N}{2} \bar{N}^C N + \text{h.c.}, \quad (\text{II.2})$$

where F_α ($\alpha = e, \mu, \tau$) and M_N are Yukawa coupling constants and Majorana mass, respectively. After breaking of EW symmetry, the sterile neutrino is mixed with active neutrinos. The degree of mixing is characterized by the active-sterile mixing denoted as $V_\alpha \equiv M_D/M_N = (F_\alpha \langle H \rangle)/M_N$. Sterile neutrino can decay into 3ν or $\nu \ell^+ \ell^-$ through this mixing. Inversely, if sterile neutrino is relatively light, for instance $M_N < m_\pi$, it can be produced by the decay of light mesons. In this case, we can find the signal of sterile neutrino as a different peak in the energy spectrum of ordinary neutrinos.

Under this assumption, the energy spectrum of e^\pm , *i.e.*, $d\Gamma/dE_e$ is calculated (Appendix A), and input in Eq. (II.1). In this paper, we fix parameters of the sterile neutrino as one possible simple example case as follows. The sterile neutrino couples to charged or neutral currents of the electron flavor only. The strengths of the coupling of N to the currents are then given by $|V_e| \equiv \Theta$ and $|V_\mu| = |V_\tau| = 0$.

D. primary photon spectrum

We assume that energetic e^\pm 's are injected at the N decay. Energetic photons are then produced via the inverse-Compton scattering between the e^\pm 's and CBR ($e^\pm + \gamma_{\text{bg}} \rightarrow e^\pm + \gamma$). The inverse-Compton process plays an important role in developments of electromagnetic cascade shower. It distributes the energy of e^\pm generated at the decay to multiple particles, *i.e.*, photons γ and electrons and positrons e^\pm in the thermal bath. We assume that the e^\pm in the initial state with energy E_e reacts with CBR with energy $E_{\gamma \text{b}}$, and scattered photon in the final state has energy of $E_{\gamma 0}$. Number of collisions for an e^\pm particle per unit time dt and unit energy interval of photon in the final state $dE_{\gamma 0}$ is then approximately given [36, 59] [79] by

$$\frac{d^2 N}{dt dE_{\gamma 0}} = \frac{2\pi r_e^2 m_e^2}{E_{\gamma \text{b}} E_e^2} F(E_{\gamma 0}, E_e, E_{\gamma \text{b}}), \quad (\text{II.3})$$

where m_e is the electron mass, $r_e = \alpha/m_e$ is the classical radius of electron with the fine structure constant α , and the function $F(E_{\gamma 0}, E_e, E_{\gamma \text{b}})$ is defined by

$$F(E_{\gamma 0}, E_e, E_{\gamma \text{b}}) = \begin{cases} 2q \ln q + (1+2q)(1-q) + \frac{(\gamma_E q)^2}{2(1+\gamma_E q)}(1-q) & \text{for } 0 < q \leq 1 \\ 0 & \text{otherwise,} \end{cases} \quad (\text{II.4})$$

where parameters are introduced as

$$\gamma_E = \frac{4E_{\gamma \text{b}} E_e}{m_e^2}, \quad q = \frac{E_{\gamma 0}}{\gamma_E (E_e - E_{\gamma 0})}. \quad (\text{II.5})$$

The energy spectrum of CBR in the early universe is almost completely described by a Planck distribution,

$$f_{\gamma \text{b}}(E_{\gamma \text{b}}) = \frac{E_{\gamma \text{b}}^2}{\pi^2} \frac{1}{\exp(E_{\gamma \text{b}}/T) - 1}. \quad (\text{II.6})$$

The energy of photon in the final state has an upper limit [59],

$$E_{\gamma 0} \leq E_{\gamma 0, \max} = \frac{4E_{\gamma b}E_e^2}{m_e^2(1 + 4E_{\gamma b}E_e/m_e^2)}. \quad (\text{II.7})$$

When the maximum photon energy is between the threshold for the photodisintegration of ${}^7\text{Be}$ (1.59 MeV) and that of D (2.22 MeV), an effective destruction of ${}^7\text{Be}$ is possible without destructions of other light nuclides [30]. The maximum energy should, therefore, be in this energy range, *i.e.*, $E_{\gamma 0, \max} \sim 2$ MeV. The average energy of CBR, $\bar{E}_{\gamma b} = 2.701T$, is used for the CBR energy approximately. The e^\pm energy required for the generation of nonthermal photon with $E_{\gamma 0} \sim 2$ MeV is then estimated to be

$$E_e \gtrsim \frac{1}{2} \left(E_{\gamma 0, \max} + m_e \sqrt{\frac{E_{\gamma 0, \max}}{E_{\gamma b}}} \right) \sim 7.5 \text{ MeV} \quad (\text{for } t = 10^6 \text{ s}). \quad (\text{II.8})$$

Generally, at inverse Compton scatterings of low energy CBRs by energetic e^\pm in the early universe, small fractions of energies of e^\pm are transferred to those of CBRs at respective scatterings, *i.e.*, $E_{\gamma 0} \lesssim E_e$. The energy spectrum of the primary photon produced at the inverse Compton scattering is, therefore, approximated to be proportional to the differential scattering rate as a function of $E_{\gamma 0}$. The spectrum of the primary photon is then given by

$$P_{\text{IC}}(E_e, E_{\gamma 0}, T) = \frac{F(E_{\gamma 0}, E_e, E_{\gamma b})}{\int F(E_{\gamma 0}, E_e, E_{\gamma b}) dE_{\gamma 0}} = \frac{F(E_{\gamma 0}, E_e, E_{\gamma b})}{\frac{E_e}{\gamma_E} \left[\frac{8+9\gamma_E+\gamma_E^2}{2\gamma_E} \ln(1+\gamma_E) - \frac{16+18\gamma_E+\gamma_E^2}{4(1+\gamma_E)} + 2\text{Li}_2(-\gamma_E) \right]}, \quad (\text{II.9})$$

where $\text{Li}_2(-x)$ is the dilogarithm. The dilogarithm is calculated in our code using the published Algorithm 490 [60].

E. electromagnetic cascade

The energetic primary photons interact with the CBR, and electromagnetic cascade shower composed of energetic photons and e^\pm develops (*e.g.*, [32, 36]). One energetic photon can produce multiple particles of lower energies by continuous reactions of pair production at a collision with CBR $\gamma_{\text{bg}} (\gamma + \gamma_{\text{bg}} \rightarrow e^+ + e^-)$ and inverse Compton scattering of e^\pm at a collision with CBR ($e^\pm + \gamma_{\text{bg}} \rightarrow e^\pm + \gamma$). The non-thermal photons then obtain a quasi-static equilibrium spectrum [36, 61].

When the energy of the primary photon $E_{\gamma 0}$ is much larger than the threshold energy of photodisintegration of light nuclides, *i.e.*, $E_{\gamma 0} \gg 1$ MeV, the steady state energy spectrum of the nonthermal photons is approximately given (*e.g.*, [39, 43, 62]) by

$$p_{\gamma, \text{EC}}(E_\gamma, E_{\gamma 0}, T) = \begin{cases} K(E_X/E_\gamma)^{3/2} & \text{for } E_\gamma \leq E_X, \\ K(E_X/E_\gamma)^2 & \text{for } E_X < E_\gamma \leq E_C, \\ 0 & \text{for } E_C \leq E_\gamma, \end{cases} \quad (\text{II.10})$$

where $E_X \sim m_e^2/(80T)$ and $E_C \sim m_e^2/(22T)$ [36] are the energy corresponding to a break in the power law, and a cutoff energy, respectively, $K = E_{\gamma 0}/\{E_X^2[2 + \ln(E_C/E_X)]\}$ is the normalization constant which conserves the energy of the primary photon. If nonthermal photons have energies larger than E_C , they are quickly destroyed via electron-positron pair production.

The maximum energy of the non-thermal photon $E_{\gamma 0}$, however, can be of the order of $\mathcal{O}(1\text{MeV})$. In this case, the generalized photon spectrum is given [30] as follows: (1) For $E_{\gamma 0} \leq E_X$, the spectrum is given by

$$p_{\gamma, \text{EC1}}(E_\gamma, E_{\gamma 0}, T) = \begin{cases} K_1(E_X/E_\gamma)^{3/2} & \text{for } E_\gamma \leq E_{\gamma 0}, \\ 0 & \text{for } E_{\gamma 0} < E_\gamma, \end{cases} \quad (\text{II.11})$$

where $K_1 = E_{\gamma 0}^{1/2}/(2E_X^{3/2})$.

(2) For $E_X < E_{\gamma 0} \leq E_C$, the spectrum is given by

$$p_{\gamma, \text{EC2}}(E_\gamma, E_{\gamma 0}, T) = \begin{cases} K_2(E_X/E_\gamma)^{3/2} & \text{for } E_\gamma \leq E_X, \\ K_2(E_X/E_\gamma)^2 & \text{for } E_X < E_\gamma \leq E_{\gamma 0}, \\ 0 & \text{for } E_{\gamma 0} < E_\gamma, \end{cases} \quad (\text{II.12})$$

where $K_2 = E_{\gamma 0}/\{E_X^2[2 + \ln(E_{\gamma 0}/E_X)]\}$.

(3) For $E_C < E_{\gamma 0}$, the spectrum $p_{\gamma, \text{EC3}}(E_\gamma, E_{\gamma 0}, T)$ is given as Eq. (II.10).

F. steady state spectrum

Rates of electromagnetic interactions are faster than the cosmic expansion rate. The injection spectrum $p_\gamma(E_\gamma, T, M_N)$ is then quickly modified to a new quasi-static equilibrium spectrum given by

$$\mathcal{N}_\gamma^{\text{QSE}}(E_\gamma, T, M_N) = \frac{n_N p_\gamma(E_\gamma, T, M_N)}{\Gamma_\gamma(E_\gamma) \tau_N}, \quad (\text{II.13})$$

where $n_N = n_N^0(1+z)^3 \exp(-t/\tau_N)$ is the number density of the decaying particles N at a redshift z . The quantity Γ_γ is the energy degradation rate of nonthermal photon through three relatively slow processes; Compton scattering ($\gamma + e_{\text{bg}}^\pm \rightarrow \gamma + e^\pm$), Bethe-Heitler ordinary pair creation in nuclei ($\gamma + N_{\text{bg}} \rightarrow e^+ + e^- + N$), and double photon scattering ($\gamma + \gamma_{\text{bg}} \rightarrow \gamma + \gamma$) for the zeroth-generation nonthermal photons. We use this steady state approximation for the non-thermal photon component.

G. nonthermal nucleosynthesis

If the injection of non-thermal photons occurs at a cosmic time $t \gtrsim 10^4$ s, the nonthermal photons can disintegrate background nuclei, and nuclear abundances can be changed [31–43, 63]. The equation describing a time evolution of nuclear abundance is given by

$$\frac{dY_A}{dt} = \sum_T N_{AC} [T\gamma]_A Y_T - \sum_P [A\gamma]_P Y_A, \quad (\text{II.14})$$

where we define the reaction rate

$$\begin{aligned} [T\gamma]_A &= \frac{n_\gamma^0 \zeta_{N \rightarrow e}}{\tau_N} \left(\frac{1}{2H_r t} \right)^{3/2} \exp(-t/\tau_N) \\ &\times \int_0^\infty dE_\gamma S_\gamma^{\text{QSE}}(E_\gamma, T, M_N) \sigma_{\gamma+T \rightarrow A}(E_\gamma), \end{aligned} \quad (\text{II.15})$$

and

$$S_\gamma^{\text{QSE}}(E_\gamma, T, M_N) = \frac{\tau_N}{E_{\gamma 0} n_N} \mathcal{N}_\gamma^{\text{QSE}}(E_\gamma, T, M_N). \quad (\text{II.16})$$

$Y_i \equiv n_i/n_B$ is the mole fraction of a nuclear species i , and n_i and n_B are number densities of nuclei i and total baryon, respectively. The first and second term on the right-hand side in Eq. (II.14) correspond to the production ($\gamma + T \rightarrow A + C$) and destruction ($\gamma + A \rightarrow P + D$), respectively, for nuclide A . E_γ is the energy of non-thermal photon which triggers the photodisintegration. The cross section of the process $\gamma + T \rightarrow A + C$ is denoted by $\sigma_{\gamma+T \rightarrow A}(E_\gamma)$. In addition, we use N_{AC} as the number of identical nuclear species in a production or destruction process; $N_{AC} = 2$ when particles A and C are identical and $N_{AC} = 1$ when they are not. For example, in the process ${}^4\text{He}(\gamma, d)\text{D}$, $N_{\text{DD}} = 2$. We defined $H_r \equiv \sqrt{8\pi G \rho_{\text{rad}}^0/3}$, where the superscript 0 denotes present values (redshift $z = 0$). n_γ^0 and ρ_{rad}^0 are, therefore, the present number density of CBR and present radiation energy density, respectively. Furthermore, we defined $\zeta_{N \rightarrow e} = (n_N^0/n_\gamma^0)E_{N \rightarrow e}$.

Non-thermal nuclei produced in the primary reaction can in general experience secondary non-thermal nuclear reactions. We, however, focus on an injection of photons with relatively small energies. In this case, secondary reactions do not occur since the energies of photons responsible for secondary reactions are large. See Ref. [43] for the equation describing a secondary production and destruction which takes into account an energy loss of nuclear species operating during the propagation in the background universe.

III. RESULTS

A. Nonthermal photon spectra

Figure 1 shows energy spectra of electron [Eq. (A.6)] and positron [Eq. (A.7)] generated at the N decay, and the total spectrum (multiplied by 1/2) as a function of x_e . For all figures in this subsection, we assume that the

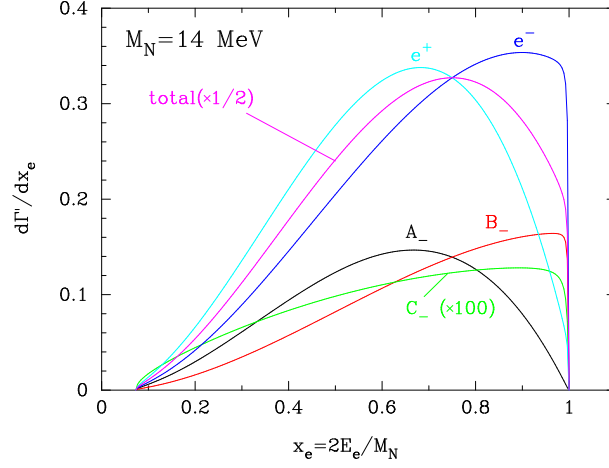


FIG. 1: Energy spectra of electron [Eq. (A.6)] and positron [Eq. (A.7)] generated at the N decay, and the total spectrum. Functional shapes of terms A , B and C [cf. Eq. (A.15)] are also shown. The mass of the sterile neutrino is assumed to be $M_N = 14 \text{ MeV}$.

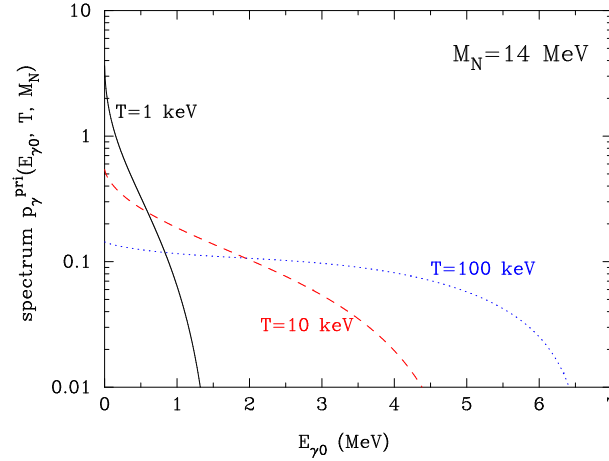


FIG. 2: Energy spectra of primary photon produced via the inverse Compton scattering of electron and positron which are generated at the decay for the cosmic temperature of $T = 1, 10$ and 100 keV . The mass of the sterile neutrino is assumed to be $M_N = 14 \text{ MeV}$.

mass of the sterile neutrino is $M_N = 14 \text{ MeV}$ since we find that this mass region is the most important for ${}^7\text{Be}$ photodisintegration in the present model (see Sec. III B). Functional shapes of terms A , B and C [cf. Eq. (A.15)] are also shown. Because of these extended energy spectra of e^{\pm} , nonthermal photons produced via inverse Compton scattering of CBR by the generated e^{\pm} also have extended energy spectra.

Figure 2 shows energy spectra of primary photon produced via the inverse Compton scattering of electron and positron which are generated at the decay for the cosmic temperature of $T = 1, 10$ and 100 keV . The primary photon spectra is given by

$$p_{\gamma}^{\text{pri}}(E_{\gamma 0}, T, M_N) = \frac{1}{\Gamma} \int_{m_e}^{M_N/2} \frac{d\Gamma}{dE_e} (M_N) P_{\text{IC}}(E_e, E_{\gamma 0}, T) dE_e. \quad (\text{III.1})$$

When the energy injection with a given spectra (Fig. 1) occurs at lower temperatures, the inverse Compton scattering produces softer spectra of nonthermal primary photon, and cutoff energies are lower [cf. Eq. (II.7); not seen in this Figure]. These results reflect the differential inverse Compton scattering rate [Eq. (II.9)].

Figure 3 shows injection spectra of nonthermal photon formed through the electromagnetic cascade calculated with Eq. (II.1) for $T = 1, 3$ and 10 keV . As the temperature decreases, the primary photon spectrum becomes soft. The photon spectrum induced by the primary photons, on the other hand, has upper cutoff at $E_C \sim m_e^2/(22T)$ [36] which

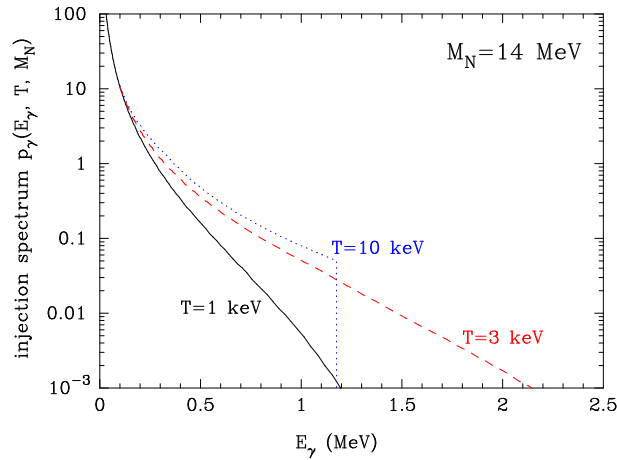


FIG. 3: Injection spectra of nonthermal photon formed through the electromagnetic cascade for $T = 1, 3$ and 10 keV. The mass of the sterile neutrino is assumed to be $M_N = 14$ MeV.

scales as inverse of the temperature. The cutoff can be seen at $E_\gamma = 1.2$ MeV for $T = 10$ keV. Because of the two reasons, there is a best temperature of the energy injection where relatively large abundances of energetic photons are produced with $E_\gamma > 1.59$ MeV which can destroy ${}^7\text{Be}$. One can find that the best temperature is 3 keV among the three temperatures.

B. light element abundances

We constrain the model of the decaying sterile neutrino by comparing calculated results and observational constraints on elemental abundances. In this model, ${}^7\text{Be}$ is disintegrated by nonthermal photons originating from the decay of sterile neutrino. Since a primordial abundance of ${}^7\text{Li}$ is mainly contributed from that of ${}^7\text{Be}$ produced during the BBN epoch, the destruction of ${}^7\text{Be}$ reduces the final ${}^7\text{Li}$ abundance. However, the energies of nonthermal photons should be small since energetic photons can disintegrate other nuclei and result in an inconsistency with observed abundances. In the case of low energy photons, abundances of only D and ${}^7\text{Be}$ can be significantly affected because of their small threshold energies for photodisintegration [30]. Constraints on the primordial abundances of D and ${}^7\text{Li}$ are, therefore, given here although nonthermal nuclear reactions of other nuclei have been included in our calculation code.

We use the primordial D abundance determined from observations of quasi-stellar object (QSO) absorption systems. As a conservative constraint, the 2σ range estimated with the mean value of ten Lyman- α absorption systems, $\log(\text{D}/\text{H}) = -4.58 \pm 0.02$ [64], is adopted: $2.40 \times 10^{-5} < \text{D}/\text{H} < 2.88 \times 10^{-5}$. Primordial ${}^7\text{Li}$ abundance is taken from a determination by spectroscopic observations of MPSs. The observed abundances are different from theoretical values in the SBBN model by a factor of about three. We adopt the observational limit, $\log({}^7\text{Li}/\text{H}) = -12 + (2.199 \pm 0.086)$ derived in a 3D nonlocal thermal equilibrium model [16]. Taking account of 2σ uncertainty, the constraint is $1.06 \times 10^{-10} < {}^7\text{Li}/\text{H} < 2.35 \times 10^{-10}$. As another possible case, we consider the case that ${}^7\text{Li}$ abundances in surfaces of MPSs are depleted by a factor of two as suggested by calculations of a stellar model with a turbulent mixing [27–29].

Figure 4 shows contours for calculated abundances of D and ${}^7\text{Li}$ in the $(\tau_N, \zeta_{N \rightarrow e})$ plane for $M_N = 14$ MeV. The solid and dotted curves for D show observational 2σ and 4σ limits, respectively. The regions above the curves are excluded by underproduction of D. Two solid lines and two dashed lines for ${}^7\text{Li}$ show the observational abundance constraints when we assume a ${}^7\text{Li}$ depletion by a factor of 1 and 2, respectively. Inside the band between two solid (dashed) lines, the calculated ${}^7\text{Li}$ abundance is consistent with the observational constraint for the case of no depletion (depletion by a factor of two) of ${}^7\text{Li}$. The ${}^7\text{Li}$ abundance is smaller in a region above the band, while it is larger in a region below. The region above the line labeled as “entropy” is excluded from the constraint on the baryon density from the WMAP measurement of CMB.

A region of long lifetime $\tau_N \gtrsim 10^6$ s is, however, excluded from observations of CBR energy spectrum. An injection of nonthermal photons to the thermal bath triggers a deformation of the CBR spectrum from black-body [65]. Such a deformation is severely constrained by observations which indicate a nearly complete Planck spectrum [66, 67]. We adopt most stringent and reliable limits on the CBR energy spectrum as follows. The limit on the chemical potential is taken from the analysis of the data from the Far-InfraRed Absolute Spectrophotometer on board the

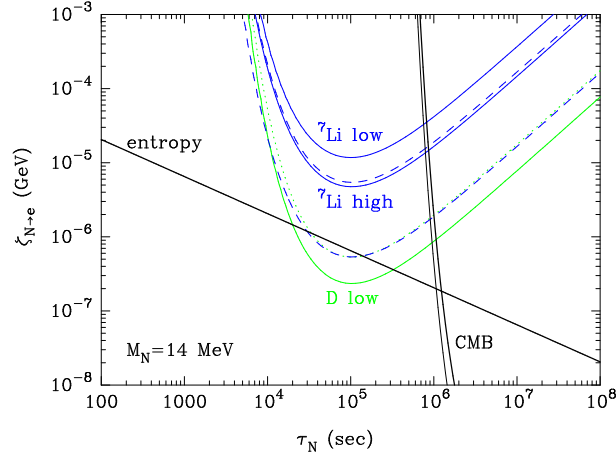


FIG. 4: Contours for calculated abundances of D and ${}^7\text{Li}$ on the parameter plane of $(\tau_N, \zeta_{N \rightarrow e})$ for $M_N = 14$ MeV. The regions above the solid and dotted curves for D are excluded by underproduction of D compared to the observational constraints at 2σ and 4σ levels, respectively. In the band between two solid lines for ${}^7\text{Li}$, the observational abundance constraint is satisfied. The ${}^7\text{Li}$ abundance is smaller in a region above the band, while it is larger in a region below. In the band between two dashed lines, the calculated ${}^7\text{Li}$ abundance is consistent with the observational constraint if ${}^7\text{Li}$ is depleted in stellar surfaces by a factor of two. The region above the line labeled as “entropy” is excluded from the constraint on the entropy production by the N decay from the WMAP CMB measurement. In addition, the right regions from the thick and thin solid lines labeled as “CMB” are excluded from the present and planned limits, respectively, on the energy spectrum of CMB.

COsmic Background Explorer, $|\mu| < 9 \times 10^{-5}$ [67]. The limit on the Compton y -parameter is taken from an updated constraint from the second generation of the Absolute Radiometer for Cosmology, Astrophysics, and Diffuse Emission (ARCADE) [80] utilizing a better fitting procedure, $|y| < 1 \times 10^{-4}$ [66]. For comparison, we also adopt planned limits of ARCADE, *i.e.*, $|\mu| < 2 \times 10^{-5}$ and $|y| < 1 \times 10^{-6}$. The right regions from the thick and thin solid lines labeled as “CMB” are excluded from the present and planned limits, respectively, on the energy spectrum of CMB. We note that in the parameter region shown in Fig. 4, this model is constrained exclusively from the limit on the CMB μ parameter.

The parameter region for small ${}^7\text{Li}$ abundance is found at $\zeta_{N \rightarrow e} \sim 10^{-6}$ GeV and $\tau \sim 10^5$ s. In the epoch after the BBN and before the matter radiation equality, the temperature in the universe T is related to the cosmic age t as $T = 1.15 \text{ keV } (t/10^6 \text{ s})^{-1/2}$. If the N decay occurs when the cosmic temperature is $\mathcal{O}(1 \text{ keV})$, the ${}^7\text{Li}$ abundance is reduced most effectively although some amount of D destruction always occurs simultaneously. The shapes of contours for D and ${}^7\text{Li}$ are explained as follows. At small values of $\tau_N \lesssim 10^4$ s, the upper cutoff of the nonthermal photon spectrum $E_C \sim m_e^2/(22T)$ [36] is smaller than threshold energies for photodisintegration of light nuclides $E_{\text{th}} \sim \mathcal{O}(1 - 10) \text{ MeV}$. Effects of nonthermal photons on elemental abundances are, therefore, negligibly small. At large values of $\tau_N \gtrsim 10^5$ s, on the other hand, primary photons produced via the inverse Compton scattering have soft energy spectra and lower cutoff energy originating from the maximum energy of the scattered photon [Eq. (II.7)]. Abundances of nonthermal photons which are enough energetic to destroy D and ${}^7\text{Li}$ are then smaller. Resultingly, effects of nuclear photodisintegration are less efficient in the long lifetime region also.

The lower dashed line overlaps with the dotted line in the allowed parameter region below the curves of the entropy and the CMB energy spectrum. It means that on these lines the ${}^7\text{Be}$ photodisintegration can reduce the primordial abundance of ${}^7\text{Li}$ down to the observed level multiplied by the depletion factor of two. The D abundance, however, simultaneously decreases down to the observational 2σ lower limit. We then find that there is no parameter region in which primordial ${}^7\text{Li}$ abundance can be reduced to the MPS value without assuming a stellar depletion. This model, however, provides a mechanism of ${}^7\text{Li}$ reduction by some small factor with its signatures imprinted in primordial D abundance, the baryon-to-photon ratio (Sec. III C) and effective neutrino number (Sec. III D).

Figures 5 and 6 show contours for calculated abundances of D and ${}^7\text{Li}$ and constraints from the baryon density and the CMB energy spectrum similar to Fig. 4 but for $M_N = 13$ and 15 MeV, respectively. From a comparison of Figures 4–6 we find that the mass of $M_N = 14$ MeV is the best case for ${}^7\text{Be}$ reduction that is a solution to the Li problem. If the mass is smaller (Fig. 5), the energy fraction of energetic photons capable of destroying ${}^7\text{Be}$ to total nonthermal photons is smaller. We then require a higher total energy generated at the N decay. This small mass case is, therefore, constrained from the CMB observation more severely. If the mass is larger (Fig. 6), on the other hand, the total energy necessary for the ${}^7\text{Be}$ photodisintegration is smaller. The efficiency of photodisintegration of D is,

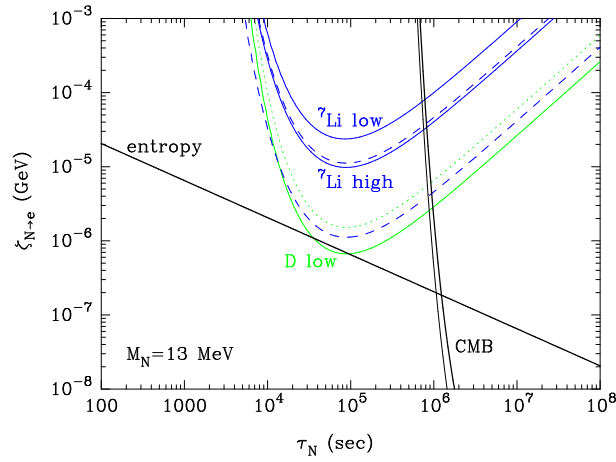


FIG. 5: Same as in Fig. 4 for $M_N = 13$ MeV.

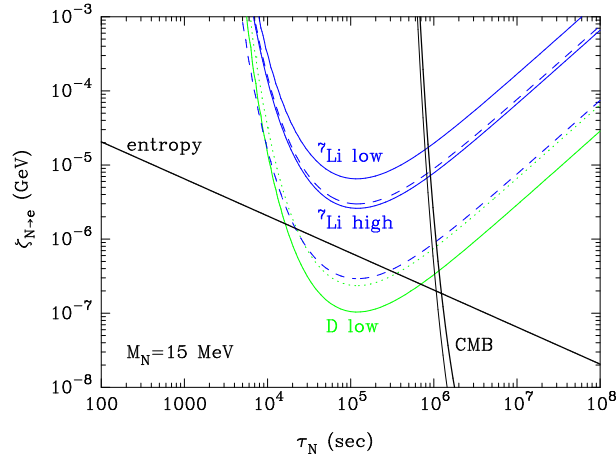


FIG. 6: Same as in Fig. 4 for $M_N = 15$ MeV.

however, relatively higher compared to that of ${}^7\text{Be}$ because of more abundant energetic photons in the nonthermal photon spectra for higher M_N . For this reason, there is no parameter region in which a ${}^7\text{Be}$ destruction occurs without too much a D destruction. In this way, we find a best mass region of $M_N = 14$ MeV. Since the parameter region for the small ${}^7\text{Li}$ abundance is about to be excluded from observational constraint from CMB energy spectrum, this model for the ${}^7\text{Li}$ reduction will be verified through the baryon-to-photon ratio and the effective neutrino number in near future.

C. baryon-to-photon ratio

An injection of energetic e^\pm increases the energy of CBR. The baryon-to-photon number ratio η is then changed by the injection as a function of cosmic time [68]. The production of nonthermal photons in electromagnetic cascade showers associated with the sterile neutrino decay enhances the comoving entropy of photon in the universe. Since the baryon-to-photon ratio is inversely proportional to the comoving photon entropy, it is reduced during the nonthermal photon injection. In order to constrain the entropy change, we use the baryon-to-photon ratio inferred from WMAP measurement of CBR which predicts primordial light element abundances consistent with observations excepting that of ${}^7\text{Li}$. If the comoving photon entropy (S_γ) changes by a small fraction, the ratio of comoving entropies measured before and after the N decay, *i.e.*, $S_{\gamma i}$ and $S_{\gamma f}$, is approximately given [68] by

$$\frac{S_{\gamma f}}{S_{\gamma i}} = \exp \left[\frac{45^{3/4} \zeta(3)}{\pi^{11/4}} \frac{(g_*^{\tau_N})^{1/4}}{g_{\gamma*S}^i} \frac{E_{N \rightarrow e} n_N^i}{n_\gamma^i} \sqrt{\frac{\tau_N}{M_{\text{Pl}}}} \right], \quad (\text{III.2})$$

where $\zeta(3) = 1.202$ is the zeta function, $g_*^{\tau_N} = 3.36$ is the relativistic degree of freedom after the BBN epoch in terms of number, and $g_{\gamma*S}^i = g_\gamma = 2$ is the relativistic degrees of freedom after the BBN epoch in terms of entropy, which is the same as statistical degrees of freedom of photon [81]. n_N^i and n_γ^i are number densities of the decaying particle and photon, respectively, evaluated at the same time before the decay; and $M_{\text{Pl}} = 1.22 \times 10^{19}$ GeV is the Planck mass. For a small fractional change of entropy, this value is given [68] by

$$\frac{\Delta S}{S} \approx \ln \frac{S_f}{S_i} = 2.14 \times 10^{-4} \left(\frac{\zeta_{N \rightarrow e}}{10^{-9} \text{ GeV}} \right) \left(\frac{\tau_N}{10^6 \text{ s}} \right)^{1/2}, \quad (\text{III.3})$$

The 2σ uncertainty from the $\Omega_b h^2$ value measured by WMAP [7] corresponds to a constraint on the change in comoving entropy by a factor of 0.044.

D. effective neutrino number

The decay of sterile neutrino has two effects on resulting value of effective neutrino number in the universe, *i.e.*, N_{eff} . Firstly, since the decay generates energetic neutrinos, the total energy density of neutrino increases with respect to the case of no neutrino injection at the decay. Secondly, since the decay also generates energetic electron and positron, the energy density of background photon increases. The ratio between energy densities of neutrino and photon is, therefore, reduced, and resulting effective neutrino number is reduced compared to the case of no photon injection.

1. energy injection

In this study, we assume that the decay lifetime of the sterile neutrino is much larger than the time scale of the decoupling of the active neutrino in the early universe, *i.e.*, $t \gg 1$ s. The energetic neutrino generated at the decay cannot interact effectively with background particles mainly constituted of weakly interacting neutrinos and weakly-noninteracting photon. The energetic neutrino is then never thermalized, and propagates in the universe without collisions. The change of the energy density of active neutrino triggered by the decay can, therefore, be formulated as in the case of that of photon by a nonthermal photon injection in the late universe. We assume that the change in the total radiation energy density by the decay is relatively small so that the cosmic expansion rate is not affected so much. The standard radiation dominated universe is then assumed approximately. When we do not take into account the nonthermal photon injection at the N decay, then the ratio between the increase of energy density of active neutrino to the energy density of photon is given [65] by

$$\frac{\Delta \rho_\nu}{\rho_{\gamma i}} = \frac{\zeta_{N \rightarrow \nu}}{2.70 T_i(t_{\text{eff}})}, \quad (\text{III.4})$$

where the effective time is defined as $t_{\text{eff}} = [\Gamma(1 + \beta)]^{1/\beta} \tau_N$ for the universe with the time-temperature relation of $T \propto t^{-\beta}$ with $\Gamma(x)$ the gamma function of argument x [82]. The quantity $\zeta_{N \rightarrow \nu} = (n_N^0/n_\gamma^0) E_{N \rightarrow \nu}$ was defined with $E_{N \rightarrow \nu}$ the average energy of active neutrino emitted at one N decay event. For the radiation dominated universe considered here, $\beta = 1/2$ and $t_{\text{eff}} = (\pi/4) \tau_N$ are satisfied.

In the case of no injection of nonthermal photon, the change in the neutrino energy density and the energy density of photon are described as

$$\Delta \rho_\nu = \frac{7}{8} \frac{\pi^2}{30} 2 \Delta N_{\text{eff},i} \left(\frac{4}{11} \right)^{4/3} T_i^4, \quad (\text{III.5})$$

$$\rho_{\gamma i} = \frac{\pi^2}{30} 2 T_i^4, \quad (\text{III.6})$$

where $\Delta N_{\text{eff},i}$ is the increase of the effective neutrino number caused by the nonthermal active neutrino injection under the assumption of no injection of nonthermal photon. From Eqs. (III.4), (III.5), and (III.6), we find that the

$\Delta N_{\text{eff},i}$ value is related to the parameter $\zeta_{N \rightarrow \nu}$ as

$$\Delta N_{\text{eff},i} = \frac{8}{7} \left(\frac{11}{4} \right)^{4/3} \frac{\zeta_{N \rightarrow \nu}}{2.70 T_i(t_{\text{eff}})}. \quad (\text{III.7})$$

When effects of nonthermal photon injection are not considered, the effective neutrino number normalized to the primordial CBR is then $N_{\text{eff},i} = 3 + \Delta N_{\text{eff},i}$.

2. dilution

The entropy of the universe is increased by the injection of nonthermal electron and positron at the N decay. As a result, the number and energy densities of neutrino for a fixed photon temperature T are decreased compared to the case of no entropy production. The effective number is then given by

$$\Delta N_{\text{eff}} = \Delta N_{\text{eff},i} \left(\frac{a_f}{a_i} \right)^{-4} \frac{T_i^4}{T_f^4} = \Delta N_{\text{eff},i} \left(\frac{S_f}{S_i} \right)^{-4/3}. \quad (\text{III.8})$$

For example, N_{eff} value for parameters $(\tau_N, \zeta_{N \rightarrow e}) = (10^5 \text{ s}^{-1}, 5 \times 10^{-7} \text{ GeV})$ in the case of $M_N = 14 \text{ MeV}$ is estimated as follows. This decay lifetime corresponds to $t_{\text{eff}} = 7.85 \times 10^4 \text{ s}$ and $T(t_{\text{eff}}) = 4.10 \text{ keV}$. This N decay increases the entropy and resultingly the baryon-to-photon ratio during the BBN epoch up to near the 2σ upper limit [Eq. (III.3) and Fig. 4]. The effective number is then increased to $N_{\text{eff},i} = 3.64$ by the following estimation.

In the present model, the sterile neutrino has only two decay modes, *i.e.*, $N \rightarrow \nu_e e^+ e^-$ and $N \rightarrow \sum_{\beta} \nu_e \bar{\nu}_{\beta} \nu_{\beta}$. The ratio of the decay rates for the two modes is defined with Eqs. (A.9) and (A.21) as

$$R_{\text{dec}} = \frac{\Gamma(N \rightarrow \nu_e e^+ e^-)}{\Gamma(N \rightarrow \sum_{\beta} \nu_e \bar{\nu}_{\beta} \nu_{\beta})}. \quad (\text{III.9})$$

Through the two decay modes, energetic neutrinos, electrons, and positrons are generated. The ratio of total energies injected in the forms of ν (including all flavors and antineutrinos) and e^{\pm} through the two decay modes is given by

$$R(\nu, e) = \frac{1 + R_{\text{dec}} f_E(\nu_e)}{R_{\text{dec}} [f_E(e^-) + f_E(e^+)]}, \quad (\text{III.10})$$

where $f_E(i) = \bar{E}_i/M_N$ is the fraction of the average energy of species i to the sterile neutrino mass in the decay mode of $N \rightarrow \nu_e e^+ e^-$, and the equation, $f_E(\nu_e) + f_E(e^-) + f_E(e^+) = 1$ is satisfied. We have a trivial relation between parameters:

$$\frac{\zeta_{N \rightarrow \nu}}{\zeta_{N \rightarrow e}} = R(\nu, e). \quad (\text{III.11})$$

The present mass corresponds to parameters of $x_e = m_e/M_N = 0.0365$ and $L = -13.236$ [Eq. (A.12)]. The ratio of decay rates is $R_{\text{dec}} = 0.575$. The fractions of the average energies in the decay mode $N \rightarrow \nu_e e^+ e^-$ are $f_E(\nu_e) = 0.348$, $f_E(e^-) = 0.308$, and $f_E(e^+) = 0.345$. Accordingly, the ratio of the energy injection is $R(\nu, e) = 3.20$. The effective number is then derived as $N_{\text{eff},i} = 3.64$ [Eqs. (III.7) and (III.11)].

Taking account of the entropy production, the final effective number is $N_{\text{eff}} = 3.48$ [Eqs. (III.3) and (III.8)]. We note that a slight change in the cosmic expansion rate through a change in g_* value due to the N decay was neglected in this estimation.

3. mixing with muon and tauon neutrinos

If either of muon or tauon neutrino predominantly couples to N and couplings of other charged leptons are negligible as an opposite extreme case, effects of the sterile neutrino decay are changed. For example, we take the case of $M_N = 14 \text{ MeV}$. The ratio of energy injections in the forms of e^{\pm} and ν is $R(\nu, e) = 3.20$ for the coupling to ν_e , while it is $R(\nu, \alpha) = 13.0$ for the coupling to ν_{α} ($\alpha = \mu$ or τ) [Eq. (III.11)]. The muon or tauon type mixings, therefore, result in a large energy fraction of neutrino emitted at the decay. A sterile neutrino that mixes only with ν_{α} thus has a small effects on BBN and the η value relative to that on N_{eff} . For this reason, no significant amount of ${}^7\text{Li}$ reduction is expected in the BBN model including a sterile neutrino which only mixes with muon or tauon neutrinos.

IV. DISCUSSIONS

A. dilution of sterile neutrino

Weak interaction rates of sterile neutrinos, N 's, with weakly interacting SM model particles after the EW phase transition scale [47] as

$$\Gamma \sim G_F^2 \Theta^2 T^5, \quad (\text{IV.1})$$

where G_F is the Fermi constant, $\Theta \approx V_{\alpha I} \ll 1$ is the mixing angle, and T is the temperature of the thermal bath. The ratio between the rates and cosmic expansion rate, H , is then given by

$$\begin{aligned} \frac{\Gamma}{H} &\sim G_F^2 \Theta^2 T^5 \left(\frac{2\pi^{3/2}}{3\sqrt{5}} \frac{g_*^{1/2} T^2}{M_{\text{Pl}}} \right)^{-1} \\ &= \frac{3\sqrt{5}}{2\pi^{3/2}} \frac{M_{\text{Pl}} G_F^2 \Theta^2 T^3}{g_*^{1/2}} \\ &= 9.69 \times 10^7 \left(\frac{\Theta}{10^{-3}} \right)^2 \left(\frac{g_*}{106.75} \right)^{-1/2} \left(\frac{T}{100 \text{ GeV}} \right)^3 \\ &= 1.00 \left(\frac{\Theta}{10^{-3}} \right)^2 \left(\frac{g_*}{63.5} \right)^{-1/2} \left(\frac{T}{0.2 \text{ GeV}} \right)^3, \end{aligned} \quad (\text{IV.2})$$

where g_* is the total massless degrees of freedom. The statistical degrees of freedom of the sterile neutrino, *i.e.*, $\Delta g_* = 2 \times 7/8$ were added to the value of $g_* = 61.75$ at $T = 200 \text{ MeV}$ in the standard model. A sterile neutrino with mixing angle $\Theta \sim 10^{-3}$ would thus freeze out from equilibrium at temperature $T \sim 200 \text{ MeV}$. The relic abundance of N is, therefore, given by the abundance fixed at $T \sim 200 \text{ MeV}$.

If a light sterile neutrino with the mass $M_N = \mathcal{O}(10) \text{ MeV}$ survives in BBN epoch, its number density must have diluted in order to realize a standard radiation dominated universe during BBN epoch. As an example, we consider the case of $M_N = 14 \text{ MeV}$, $\zeta_{N \rightarrow e} = 5 \times 10^{-7} \text{ GeV}$ and $\zeta_{N \rightarrow e}/\zeta_{N \rightarrow \nu} = 0.313$. This assumption corresponds to the total energy injection of $\zeta_N = \zeta_{N \rightarrow e} + \zeta_{N \rightarrow \nu} = 2.10 \times 10^{-6} \text{ GeV}$. This energy injection is realized by the decay of sterile neutrino with $M_N = 14 \text{ MeV}$ and the ratio between the N number density and the entropy density of $Y_N \equiv n_N/s = 2.13 \times 10^{-5}$. The ratio in the epoch of the weak reaction freeze out after the EW phase transition is, however, $Y_N = 6.56 \times 10^{-3} (g_{*S}/63.5)^{-1}$. A dilution of the sterile neutrino is needed in a epoch between the weak freeze-out [$T \sim \mathcal{O}(100) \text{ MeV}$] and the decay [$T \sim \mathcal{O}(1) \text{ keV}$].

It is shown that the decays of heavier sterile neutrinos can lead to a dilution of the light sterile neutrino ($M_N \sim 14 \text{ MeV}$) although our naive estimate [69] suggests that decays of heavier sterile neutrinos would result in dilution factors smaller than required for the appropriate abundance of light sterile neutrino by some factor at least. The decay lifetime of sterile neutrinos is roughly given [cf. Eq. (A.9)] as

$$\begin{aligned} \Gamma(N - \text{decay}) &\sim \frac{G_F^2 \Theta^2 M_N^5}{192\pi^3} \\ &= 1.87 \times 10^{-5} \text{ s}^{-1} \left(\frac{\Theta}{10^{-3}} \right)^2 \left(\frac{M_N}{14 \text{ MeV}} \right)^5. \end{aligned} \quad (\text{IV.3})$$

We assume that one of heavier sterile neutrinos, *i.e.*, N_i , contributes to the dilution or entropy production predominantly. In addition, it is assumed that the heavy neutrino dominates in terms of energy density at its decay epoch. Supposing that N_i decays into relativistic leptons and quarks which are thermalized rapidly with respect to the cosmic expansion time-scale, the energy density of relativistic species after the decay is $\rho_R = \frac{\pi^2}{30} g_* T_{\text{RH}}^4$, where T_{RH} is the reheating temperature. This energy density equals to the energy density of N_i before the decay. The ratio of the entropy per comoving volume at the epoch long after the decay (f) to that long before the decay (i) is given [70] by

$$\begin{aligned} \frac{S_f}{S_i} &= \frac{g_{*S}(T_f) a_f^3 T_f^3}{g_{*S}(T_i) a_i^3 T_i^3} \\ &\simeq 1.83 \langle g_*^{1/3} \rangle^{3/4} \frac{m_{N_i} Y_{N_i} \tau_{N_i}^{1/2}}{M_{\text{Pl}}^{1/2}} \\ &= 8.25 \times 10^1 \left(\frac{\langle g_*^{1/3} \rangle^{3/4}}{104^{1/4}} \right) \left(\frac{m_{N_i}}{100 \text{ GeV}} \right) \left(\frac{Y_{N_i}}{4.00 \times 10^{-3}} \right) \left(\frac{\tau_{N_i}}{10^{-2} \text{ s}} \right)^{1/2}, \end{aligned} \quad (\text{IV.4})$$

where a_j and T_j (for $j=i$ and f) are the scale factor and the temperature of the universe at time j , and we supposed $g_* = g_{*S}$ and that the g_* and g_{*S} values do not change between the temperatures of T_i and T_f . From this equation we find that the dilution factor, that equals the entropy enhancement factor, is about a factor of 100 at maximum. This maximum factor is smaller than a necessary factor of 300 by a factor of ~ 3 . Some mechanism for the dilution is, therefore, needed for the light sterile neutrino to destroy some moderate fraction of primordial ${}^7\text{Be}$ successfully.

B. constraint from pion decay

We assume the mass of sterile neutrino to be 14 MeV. If the lifetime is $\sim 10^5$ s (parameter value for the ${}^7\text{Li}$ reduction), and mixing angles of muon and tauon types, Θ_μ and Θ_τ , respectively, can be neglected, the active-sterile mixing angle is fixed as $\Theta = \mathcal{O}(10^{-3})$ [Eqs. (IV.3) and (A.9)] There is another issue if muon type mixing is sizable. At the low energy phenomena, such a sterile neutrino can be produced by the decay of charged pion, *e.g.* $\pi^+ \rightarrow \mu^+ + N$ or $\pi^+ \rightarrow e^+ + N$. This channel has been searched for a long time and many experiments gave the constraints on the active-sterile mixing angle. From Ref. [71], Θ_μ^2 should be smaller than 10^{-5} . In other words, if the precision of those experiments can be improved a few orders of the magnitude, we may see such a signal from pion decays or exclude the possibility. Furthermore, if the muon type mixing is of the order $\Theta_\mu \sim 10^{-6}$, such a sterile neutrino might be confirmed by Super Kamiokande [72]. On the other hand, it is worth mentioning that a constraint from supernova SN1987A observation provides a result [47, 48]; that is roughly, $\Theta^2 < 10^{-8}$.

V. SUMMARY

The primordial lithium abundance determined from spectroscopic observations of MPSs is smaller than the theoretical prediction of SBBN model by a factor of ~ 3 . A BBN model with a long-lived radiatively decaying exotic particle provides a solution to the Li problem. In this model nonthermal photons generated by the particle decay disintegrate ${}^7\text{Be}$. The primordial ${}^7\text{Li}$ abundance, which is the sum of abundances of ${}^7\text{Li}$ and ${}^7\text{Be}$ produced during BBN, is then reduced. In this paper, we studied the possibility of MeV sterile neutrino N . If it decays after BBN, and electron and positron e^\pm are emitted, the energetic e^\pm can produce energetic photon via the inverse Compton scattering of CBR. The solution to the Li problem is, therefore, also expected in this model. In the current major situation, recent neutrino oscillation experiments indicate no parameter space for the sterile neutrino corresponding to a mass smaller than the pion mass and the lifetime shorter than ~ 0.1 sec.

We calculated effects of sterile neutrino decay after BBN. Important observable effects are changes of primordial light element abundances, the baryon-to-photon ratio, and the effective neutrino number. First, we calculated injection spectrum of nonthermal photon generated by the N decay as a function of the mass M_N and temperature T . We took into account the energy spectra of e^\pm emitted at the decay, inverse Compton scattering of CBR by the energetic e^\pm producing primary energetic photons, and electromagnetic cascade showers induced by the primary photons. The energy spectra of e^\pm are broadly extended independent of the temperature. The energy spectra of the primary photons, on the other hand, depend significantly on the temperature, and spectra are softer in lower temperature or later Universe. The final injection spectra of nonthermal photon also depend on the temperature significantly. Abundances of energetic photons capable of disintegrating ${}^7\text{Be}$ are determined by the hardness of the primary photon spectra and the upper cutoff in the nonthermal photon due to the double photon pair annihilation. We find that the decay at $T = \mathcal{O}(1)$ keV is the only temperature region for an effective ${}^7\text{Be}$ destruction.

Second, we calculated nonthermal nucleosynthesis induced by the nonthermal photons. In this study, we corrected errors in cross sections for the reactions ${}^7\text{Be}(\gamma, \alpha){}^3\text{He}$ and ${}^7\text{Li}(\gamma, \alpha){}^3\text{H}$ adopted in previous studies (Appendix B). Amounts of energy injection in the form of e^\pm at the N decay are constrained by limits on the baryon-to-photon ratio η and CMB energy spectra determined from CMB observations. We found a parameter region of the lifetime τ_N and the amount of energy injection $\zeta_{N \rightarrow e}$, in which ${}^7\text{Be}$ is photodisintegrated and the Li problem is partially solved. We also found that the sterile neutrino mass is required to be $M_N = 14$ MeV. A lighter neutrino can not destroy any significant fraction of ${}^7\text{Be}$ via photodisintegration without violating the constraint on the η value. A heavier neutrino, on the other hand, can not destroy ${}^7\text{Be}$ without destroying D unrealistically much. The best parameter region is narrow even in the case of $M_N = 14$ MeV, and the decay lifetime is determined to be $\tau_N \sim 10^5$ s. Even in this region, the ${}^7\text{Be}$ destruction by more than a factor of three can not be realized since constraints on the D destruction and the change of the η value exclude this possibility.

Third, we calculated changes of the baryon-to-photon ratio η and the cosmological effective neutrino number N_{eff} . At the N decay, energetic active neutrinos, electrons, and positrons are generated. The energies of emitted neutrinos are never thermalized since the weak interaction has long since decoupled in the universe. The nonthermal neutrinos, therefore, contribute to the radiation energy density or the N_{eff} value. The energies of emitted e^\pm 's are, on the other

hand, quickly thermalized through interactions with CBR, and eventually transferred to CBR. The comoving entropy of the photon is, therefore, increased. Using formulae for the sterile neutrino decay (Appendix A), we quantitatively derived changes of η and N_{eff} caused by the N decay. We then found that in the best parameter region, the N decay changes not only the η value slightly but the N_{eff} value by a factor of $\Delta N_{\text{eff}} \lesssim 1$. For the moment, 2σ ranges of η and N_{eff} determined from CMB observations [7] do not indicate any effect by the sterile neutrino decay as considered in this paper. The η value is consistent with the value at the BBN epoch inferred from measurements of primordial light element abundances, and the effective neutrino number is consistent with the case of only three active neutrino, *i.e.*, $N_{\text{eff}} = 3$. Since error bars on the η and N_{eff} values are getting smaller, this model for the Li problem can be verified by future observations of the parameters η and N_{eff} .

Acknowledgments

We are grateful to Shintaro Eijima and Kazuhiro Takeda for helpful comments. This work was supported by Inoue Foundation for Science [HI].

Appendix A: formulae of sterile neutrino decay

We derive the total decay rate of sterile neutrinos, and energy spectra and average energies of electron and positron generated in the decay. The overall amplitude of the matrix element squared for the decay of $N_I \rightarrow \nu_\alpha + e^- + e^+$ is given by

$$|\mathcal{M}|^2 = 32G_F^2\Theta^2 [A(p_1 \cdot p_3)(p_2 \cdot p_4) + B(p_1 \cdot p_4)(p_2 \cdot p_3) + Cm_e^2(p_1 \cdot p_2)] \quad (\text{A.1})$$

where G_F is the Fermi constant, $\Theta \approx V_{eI} \ll 1$ is the mixing angle, p_i is the four momentum of particle i , the subscript i identifies the particle species as $i = 1$ for N_I , 2 for ν_α , 3 for e^- and 4 for e^+ , and constant parameters A , B and C are defined as

$$A = (c_V + c_A)^2, \quad (\text{A.2})$$

$$B = (c_V - c_A)^2 + 4\delta_{e\alpha} + 4(c_V + c_A)\delta_{e\alpha}, \quad (\text{A.3})$$

$$C = (c_V^2 - c_A^2) + 2(c_V - c_A)\delta_{e\alpha}, \quad (\text{A.4})$$

where $c_V = -1/2 + 2\sin^2\theta_W$ and $c_A = -1/2$ are the constants for vector and axial couplings of charged leptons to the Z^0 weak boson with $\sin^2\theta_W = 0.23$ [73] the weak angle. The A value and the first terms of B and C correspond to the Z^0 exchange, while the second term of B corresponds to the W^\pm exchange. The third term of B and the second term of C correspond to the interference contribution.

The differential decay rate as a function of energies of e^- and e^+ , *i.e.*, E_3 and E_4 , is then given by

$$\frac{d^2\Gamma}{dx_3 dx_4} = \frac{G_F^2\Theta^2 M_N^5}{64\pi^3} [Ax_3(1-x_3) + Bx_4(1-x_4) + 2Cx_m^2(2-x_3-x_4)], \quad (\text{A.5})$$

where new dimensionless variables were defined as follows: $x_m = m_e/M_N$ with m_e the electron mass, and $x_i = 2E_i/M_N$ [83].

The differential decay rates as a function of x_3 and x_4 are given [74] [84] by

$$\frac{d\Gamma}{dx_3} = \frac{G_F^2\Theta^2 M_N^5}{64\pi^3} \left\{ Ax_3(1-x_3)x_{f3} + B\left(\frac{x_{f3}^2}{2} - \frac{x_{f3}^3}{3}\right) + 2Cx_m^2 \left[(2-x_3)x_{f3} - \frac{x_{f3}^2}{2} \right] \right\}_{x_{f3}=x_{f3,-}}^{x_{f3,+}}, \quad (\text{A.6})$$

$$\frac{d\Gamma}{dx_4} = \frac{G_F^2\Theta^2 M_N^5}{64\pi^3} \left\{ A\left(\frac{x_{f4}^2}{2} - \frac{x_{f4}^3}{3}\right) + Bx_4(1-x_4)x_{f4} + 2Cx_m^2 \left[(2-x_4)x_{f4} - \frac{x_{f4}^2}{2} \right] \right\}_{x_{f4}=x_{f4,-}}^{x_{f4,+}}, \quad (\text{A.7})$$

where the terms in braces are evaluated as differences between values for $x_{fi,\pm}$ with $x_{fi,-}$ and $x_{fi,+}$ the minimum and maximum values of $x_{f\neq i}$ which is the variable to be integrated firstly. These rates are derived by integration of Eq. (A.5) over x_{fi} in the range of $x_{fi,-} \leq x_{f\neq i} \leq x_{fi,+}$. The ranges of x_3 and x_4 in Eqs. (A.6) and (A.7), respectively, are, on the other hand, $2x_m \leq x_i \leq 1$. The values $x_{fi,\pm}$ are given [74] by

$$x_{fi,\pm} = \frac{(2-x_i)(1+2x_m^2-x_i) \pm (1-x_i)\sqrt{x_i^2-4x_m^2}}{2(1+x_m^2-x_i)}. \quad (\text{A.8})$$

The total decay rate is given [74, 75] by

$$\Gamma(N \rightarrow \nu_\alpha e^+ e^-) = \frac{G_F^2 \Theta^2 M_N^5}{192\pi^3} \left\{ C_1 \left[(1 - 14x_m^2 - 2x_m^4 - 12x_m^6) \sqrt{1 - 4x_m^2} - 12x_m^4 (1 - x_m^4) L \right] \right. \\ \left. + 4C_2 \left[x_m^2 (2 + 10x_m^2 - 12x_m^4) \sqrt{1 - 4x_m^2} + 6x_m^4 (1 - 2x_m^2 + 2x_m^4) L \right] \right\}, \quad (\text{A.9})$$

where

$$C_1 = \frac{A+B}{4}, \quad (\text{A.10})$$

$$C_2 = \frac{C}{4}, \quad (\text{A.11})$$

$$L = \ln \left[\frac{1 - 3x_m^2 - (1 - x_m^2) \sqrt{1 - 4x_m^2}}{x_m^2 (1 + \sqrt{1 - 4x_m^2})} \right]. \quad (\text{A.12})$$

We adopt the weak angle of $\sin^2 \theta_W = 0.23$ [73], and $C_1 = 0.5858$ and $C_2 = 0.1679$ for the neutrino flavor of the final state $\alpha = e$.

The number spectra of the electron and positron emitted at the decay are given by

$$P_{e-}(x_3) = \frac{1}{\Gamma} \frac{d\Gamma}{dx_3}, \quad (\text{A.13})$$

$$P_{e+}(x_4) = \frac{1}{\Gamma} \frac{d\Gamma}{dx_4}. \quad (\text{A.14})$$

The total spectra of electron and positron is given by

$$P_e(x) = P_{e-}(x) + P_{e+}(x) \\ = \frac{1}{\Gamma} \frac{G_F^2 \Theta^2 M_N^5}{64\pi^3} \left\{ (A+B) \left[\frac{x_f^2}{2} - \frac{x_f^3}{3} + x_f x (1-x) \right] + 2C x_m^2 x_f (4 - 2x - x_f) \right\}_{x_f=x_{f,-}}^{x_{f,+}}. \quad (\text{A.15})$$

The average energies of electron (E_3) and positron (E_4) are given by

$$\bar{x}_3 = \frac{1}{\Gamma} \int_{2x_m}^1 x_3 \frac{d\Gamma}{dx_3} dx_3 \\ = \frac{1}{\Gamma} \frac{G_F^2 \Theta^2 M_N^5}{64\pi^3} f(A, B, C, x_m), \quad (\text{A.16})$$

$$\bar{x}_4 = \frac{1}{\Gamma} \int_{2x_m}^1 x_4 \frac{d\Gamma}{dx_4} dx_4 \\ = \frac{1}{\Gamma} \frac{G_F^2 \Theta^2 M_N^5}{64\pi^3} f(B, A, C, x_m), \quad (\text{A.17})$$

where we defined a function:

$$f(A, B, C, x_m) = A \left\{ \frac{1}{60} \sqrt{1 - 4x_m^2} (3 - 29x_m^2 + 48x_m^4 - 70x_m^6 - 60x_m^8) \right. \\ \left. - x_m^4 [(1 + x_m^2) (1 - x_m^4) L_1 + (3 - x_m^2 + x_m^4 + x_m^6) L_2] \right\} \\ - B \left\{ \frac{1}{60} \sqrt{1 - 4x_m^2} (9 - 52x_m^2 + 14x_m^4 + 80x_m^6 + 120x_m^8) \right. \\ \left. + x_m^4 [(1 - x_m^4 - 2x_m^6) L_1 + (3 + x_m^4 + 2x_m^6) L_2] \right\} \\ + C \left\{ \frac{1}{6} x_m^2 \sqrt{1 - 4x_m^2} (5 - 12x_m^2 + 10x_m^4 - 12x_m^6) \right. \\ \left. + 2x_m^4 [(1 - x_m^2) (1 - x_m^4) L_1 + (1 + x_m^2 + x_m^4 - x_m^6) L_2] \right\} \\ + (B - 2C x_m^2) \left\{ \frac{1}{24} \sqrt{1 - 4x_m^2} (5 - 38x_m^2 + 6x_m^4 + 36x_m^6) \right. \\ \left. - \frac{1}{2} x_m^4 (1 + 3x_m^4) (L_1 - L_2) \right\}, \quad (\text{A.18})$$

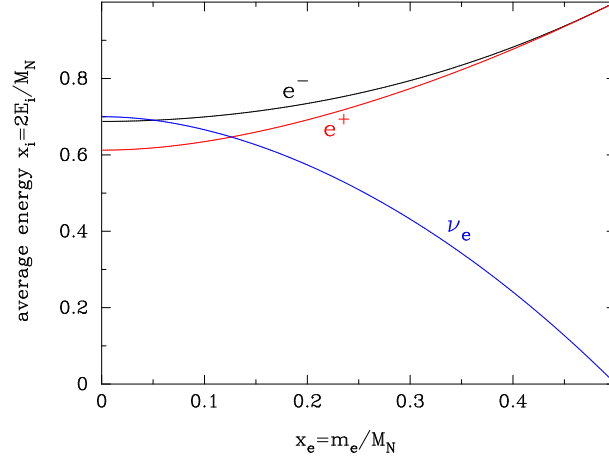


FIG. 7: Average energies of electron, positron and neutrino generated at the N decay as a function of the mass ratio of electron and sterile neutrino.

where parameters L_1 and L_2 are defined as

$$L_1 = \ln \left[\frac{1 - 3x_m^2 - (1 - x_m^2)\sqrt{1 - 4x_m^2}}{2x_m^3} \right], \quad (\text{A.19})$$

$$L_2 = \ln \left[\frac{1 + \sqrt{1 - 4x_m^2}}{2x_m} \right], \quad (\text{A.20})$$

and $L_1 - L_2 = L$ is satisfied.

Figure 7 shows average energies of electron, positron and neutrino generated at the N decay as a function of x_m calculated with Eqs. (A.16) and (A.17) and a trivial relation of $\bar{x}_2 = 2 - (\bar{x}_3 + \bar{x}_4)$. In the small x_m region, average energies of all the three particles in the final state are close to one third of the sterile neutrino mass M_N , *i.e.*, $\bar{x}_i \sim 2/3$. In the large $x_m (\lesssim 1)$ region, on the other hand, masses of electron and positron are significant fractions of the sterile neutrino mass. The most of the energy in the final state is, therefore, taken for the mass energy, and average energy of ν_e is small.

Finally, a decay rate for the mode of $N_I \rightarrow \sum_{\beta} \nu_e \bar{\nu}_{\beta} \nu_{\beta}$ is given [75] by

$$\Gamma(N \rightarrow \sum_{\beta} \nu_e \bar{\nu}_{\beta} \nu_{\beta}) = \frac{G_F^2 \Theta^2 M_N^5}{192\pi^3}. \quad (\text{A.21})$$

We note that the decay into the final state of $\nu_{\alpha} + \bar{\nu}_{\beta} + \nu_{\beta}$ for $\alpha = \mu$ and τ does not occur in the assumption adopted in this paper (see Sec. II C).

Appendix B: photodisintegration cross sections of ${}^7\text{Be}$ and ${}^7\text{Li}$

We correct significant errors in cross sections of reactions ${}^7\text{Be}(\gamma, \alpha){}^3\text{He}$ and ${}^7\text{Li}(\gamma, \alpha){}^3\text{H}$ [39] adopted in previous studies on the BBN model including the decaying X particle [30, 43, 56, 63].

A detailed balance relation between cross sections of a forward reaction $A(B, \gamma)C$ and its inverse reaction $C(\gamma, B)A$ is described [76] as

$$\sigma_{C+\gamma} = \frac{g_A g_B}{(1 + \delta_{AB}) g_C} \left(\frac{\mu E}{E_{\gamma}^2} \right) \sigma_{A+B}, \quad (\text{B.1})$$

where σ_{A+B} and $\sigma_{C+\gamma}$ are the forward and inverse reaction cross sections, respectively, $g_i = 2I_i + 1$ is the statistical degrees of freedom with spin I_i of species i , δ_{AB} is the Kronecker delta for escaping from the double counting of identical particles, μ and E are the reduced mass and the center of mass (CM) energy of the $A+B$ system, and

$E_\gamma = E + Q$ is the radiation energy with Q the reaction Q -value: $Q = 1.586627$ MeV [for ${}^3\text{He}(\alpha, \gamma){}^7\text{Be}$] and $Q = 2.467032$ MeV [for ${}^3\text{H}(\alpha, \gamma){}^7\text{Li}$], respectively.

The rate of the forward reaction is described using the Astrophysical S -factor as

$$\sigma_{A+B} = \frac{S}{E} \exp \left[-\frac{(2\mu)^{1/2} \pi Z_A Z_B \alpha}{E^{1/2}} \right], \quad (\text{B.2})$$

where Z_i is the proton number of species i , and $\alpha = 1/137.04$ is the fine structure constant. Inserting this equation in Eq. (B.1), we obtain a relation between the cross section of the inverse (photodisintegration) reaction and the S -factor of the forward (radiative capture) reaction:

$$\sigma_{C+\gamma} = \frac{g_A g_B}{(1 + \delta_{AB}) g_C} \left(\frac{\mu}{E_\gamma^2} \right) S \exp \left[-\frac{(2\mu)^{1/2} \pi Z_A Z_B \alpha}{E^{1/2}} \right]. \quad (\text{B.3})$$

S -factors for both reactions are taken from Ref. [77]. We adopted fitted functions [their Eqs. (6) and (7)] with theoretical values of $S(0) = 0.511$ keV b for ${}^7\text{Be}(\gamma, \alpha){}^3\text{He}$ and $S(0) = 0.1003$ for ${}^7\text{Li}(\gamma, \alpha){}^3\text{H}$. The photodisintegration cross sections are then given by

$$\begin{aligned} \sigma_{\tau\text{Be}+\gamma} &= \frac{409 \text{ mb}}{E_{\gamma, \text{MeV}}^2} \exp \left(-\frac{5.19}{E_{\text{MeV}}^{1/2}} \right) \exp(-0.548 E_{\text{MeV}}) \\ &\times (1 - 0.4285 E_{\text{MeV}}^2 + 0.5340 E_{\text{MeV}}^3 - 0.1150 E_{\text{MeV}}^4) \quad \text{for } Q \leq E_\gamma \leq Q + 2.1 \text{ MeV}, \end{aligned} \quad (\text{B.4})$$

where $E_{\text{MeV}} = E/\text{MeV}$ is defined, and

$$\begin{aligned} \sigma_{\tau\text{Li}+\gamma} &= \frac{80.3 \text{ mb}}{E_{\gamma, \text{MeV}}^2} \exp \left(-\frac{2.60}{E_{\text{MeV}}^{1/2}} \right) \exp(-2.056 E_{\text{MeV}}) \\ &\times (1 + 2.2875 E_{\text{MeV}}^2 - 1.1798 E_{\text{MeV}}^3 + 2.5279 E_{\text{MeV}}^4) \quad \text{for } Q \leq E_\gamma \leq Q + 1 \text{ MeV}. \end{aligned} \quad (\text{B.5})$$

It is found that both cross sections are smaller than the published values [39] by a factor of about three. It is expected that this error originates from wrong treatment of statistical degrees of freedom. We then adopt the precise cross section given above.

Another error stems from the use of the fitted functions [77] which can be reasonably applied to the cross sections only at low energy of $E_\gamma - Q \lesssim \mathcal{O}(1)$ MeV. The functions have been derived from fitting to measured data in a relatively low energy region. These functions then provide erroneous values in a large E_γ region. Especially, the function for ${}^7\text{Be}(\gamma, \alpha){}^3\text{He}$ outputs large negative value at $E_\gamma \gtrsim 5.4$ MeV. Since this error affects the final nuclear abundances calculated in the model with the X particle, we fix this. We assume constant S -factors: $S = 0.31$ keV b at $E_\gamma > Q + 2.1$ MeV for ${}^7\text{Be}(\gamma, \alpha){}^3\text{He}$ and $S = 0.06$ keV b at $E_\gamma > Q + 1$ MeV for ${}^7\text{Li}(\gamma, \alpha){}^3\text{H}$ (cf. Ref. [78]). The cross sections are then given by

$$\sigma_{\tau\text{Be}+\gamma} = \frac{248 \text{ mb}}{E_{\gamma, \text{MeV}}^2} \exp \left(-\frac{5.19}{E_{\text{MeV}}^{1/2}} \right) \quad \text{for } Q + 2.1 \text{ MeV} \leq E_\gamma, \quad (\text{B.6})$$

$$\sigma_{\tau\text{Li}+\gamma} = \frac{48.1 \text{ mb}}{E_{\gamma, \text{MeV}}^2} \exp \left(-\frac{2.60}{E_{\text{MeV}}^{1/2}} \right) \quad \text{for } Q + 1 \text{ MeV} \leq E_\gamma. \quad (\text{B.7})$$

Figure 8 shows cross sections of reactions ${}^7\text{Be}(\gamma, \alpha){}^3\text{He}$ and ${}^7\text{Li}(\gamma, \alpha){}^3\text{H}$ as a function of the photon energy. Solid and dashed lines shows values adopted in this study, which are derived by applying the detailed balance relation to polynomial fits to theoretical calculations in low [77] and high energy regions [78], respectively, for the forward radiative capture reactions. For comparison, dotted lines show fitted functions of Ref. [39].

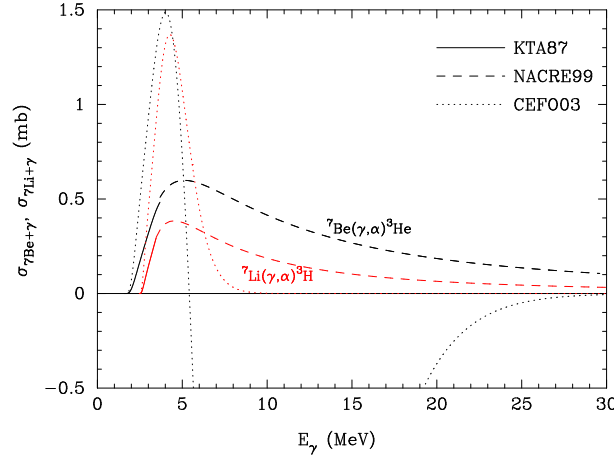


FIG. 8: Cross sections of reactions ${}^7\text{Be}(\gamma, \alpha){}^3\text{He}$ and ${}^7\text{Li}(\gamma, \alpha){}^3\text{H}$ as a function of the photon energy. Solid and dashed lines are estimated with the detailed balance relation and polynomial fits to theoretical calculations in low [77] and high energy regions [78], respectively, for the forward radiative capture reactions. Dotted lines show fitted functions of Ref. [39].

- [2] A. Coc, S. Goriely, Y. Xu, M. Saimpert and E. Vangioni, *Astrophys. J.* **744**, 158 (2012).
- [3] A. Coc, J. -P. Uzan and E. Vangioni, arXiv:1307.6955 [astro-ph.CO].
- [4] D. N. Spergel *et al.* [WMAP Collaboration], *Astrophys. J. Suppl.* **148**, 175 (2003).
- [5] D. N. Spergel *et al.* [WMAP Collaboration], *Astrophys. J. Suppl.* **170**, 377 (2007).
- [6] D. Larson *et al.*, *Astrophys. J. Suppl.* **192**, 16 (2011).
- [7] G. Hinshaw, D. Larson, E. Komatsu, D. N. Spergel, C. L. Bennett, J. Dunkley, M. R. Nolta and M. Halpern *et al.*, *Astrophys. J. Suppl.* **208**, 19 (2013).
- [8] F. Spite and M. Spite, *Astron. Astrophys.* **115**, 357 (1982).
- [9] S. G. Ryan, T. C. Beers, K. A. Olive, B. D. Fields and J. E. Norris, *Astrophys. J.* **530**, L57 (2000).
- [10] J. Melendez and I. Ramirez, *Astrophys. J.* **615**, L33 (2004).
- [11] M. Asplund, D. L. Lambert, P. E. Nissen, F. Primas and V. V. Smith, *Astrophys. J.* **644**, 229 (2006).
- [12] P. Bonifacio *et al.*, *Astron. Astrophys.* **462**, 851 (2007).
- [13] J. R. Shi, T. Gehren, H. W. Zhang, J. L. Zeng, J. L. and G. Zhao, *Astron. Astrophys.* **465**, 587 (2007).
- [14] W. Aoki, P. S. Barklem, T. C. Beers, N. Christlieb, S. Inoue, A. E. G. Perez, J. E. Norris and D. Carollo, *Astrophys. J.* **698**, 1803 (2009).
- [15] J. I. G. Hernandez, P. Bonifacio, E. Caffau, M. Steffen, H. -G. Ludwig, N. T. Behara, L. Sbordone and R. Cayrel *et al.*, *Astron. Astrophys.* **505**, L13 (2009).
- [16] L. Sbordone, P. Bonifacio, E. Caffau, H. -G. Ludwig, N. T. Behara, J. I. G. Hernandez, M. Steffen and R. Cayrel *et al.*, *Astron. Astrophys.* **522**, A26 (2010).
- [17] L. Monaco, P. Bonifacio, L. Sbordone, S. Villanova and E. Pancino, *Astron. Astrophys.* **519**, L3 (2010).
- [18] L. Monaco, S. Villanova, P. Bonifacio, E. Caffau, D. Geisler, G. Marconi, Y. Momany and H. -G. Ludwig, *Astron. Astrophys.* **539**, A157 (2012).
- [19] A. Mucciarelli, M. Salaris and P. Bonifacio, *Mon. Not. R. Astron. Soc.* **419**, 2195 (2012).
- [20] W. Aoki, H. Ito and A. Tajitsu, *Astrophys. J.* **751**, L6 (2012).
- [21] W. Aoki, *Memorie della Societa Astronomica Italiana Supplementi* **22**, 35 (2012).
- [22] P. A. R. Ade *et al.* [Planck Collaboration], arXiv:1303.5076 [astro-ph.CO].
- [23] B. D. Fields, *Ann. Rev. Nucl. Part. Sci.* **61**, 47 (2011).
- [24] C. P. Deliyannis, P. Demarque and S. D. Kawaler, *Astrophys. J. Suppl.* **73**, 21 (1990).
- [25] M. H. Pinsonneault, T. P. Walker, G. Steigman and V. K. Narayanan, *Astrophys. J.* **527**, 180 (2002).
- [26] M. H. Pinsonneault, G. Steigman, T. P. Walker and V. K. Narayans, *Astrophys. J.* **574**, 398 (2002).
- [27] O. Richard, G. Michaud and J. Richer, *Astrophys. J.* **619**, 538 (2005).
- [28] A. J. Korn *et al.*, *Astrophys. J.* **671**, 402 (2007).
- [29] K. Lind, F. Primas, C. Charbonnel, F. Grundahl and M. Asplund, *Astron. Astrophys.* **503**, 545 (2009).
- [30] M. Kusakabe, A. B. Balantekin, T. Kajino and Y. Pehlivan, *Phys. Rev D* **87**, 085045 (2013).
- [31] D. Lindley, *Mon. Not. R. Astron. Soc.* **188**, 15P (1979).
- [32] J. R. Ellis, D. V. Nanopoulos and S. Sarkar, *Nucl. Phys. B* **259**, 175 (1985).
- [33] S. Dimopoulos, R. Esmailzadeh, L. J. Hall and G. D. Starkman, *Astrophys. J.* **330**, 545 (1988).
- [34] J. Ellis, G. B. Gelmini, J. L. Lopez, D. V. Nanopoulos and S. Sarkar, *Nucl. Phys. B* **373**, 399 (1992).
- [35] M. Kawasaki and T. Moroi, *Prog. Theor. Phys.* **93**, 879 (1995).
- [36] M. Kawasaki and T. Moroi, *Astrophys. J.* **452** 506 (1995).

- [37] K. Jedamzik, Phys. Rev. Lett. **84**, 3248 (2000).
- [38] M. Kawasaki, K. Kohri and T. Moroi, Phys. Rev. D **63**, 103502 (2001).
- [39] R. H. Cyburt, J. R. Ellis, B. D. Fields and K. A. Olive, Phys. Rev. D **67**, 103521 (2003).
- [40] M. Kawasaki, K. Kohri and T. Moroi, Phys. Rev. D **71**, 083502 (2005).
- [41] J. R. Ellis, K. A. Olive and E. Vangioni, Phys. Lett. B **619**, 30 (2005).
- [42] K. Jedamzik, Phys. Rev. D **74**, 103509 (2006).
- [43] M. Kusakabe, T. Kajino and G. J. Mathews, Phys. Rev. D **74**, 023526 (2006).
- [44] M. Fukugita and T. Yanagida, Phys. Lett. B **174**, 45 (1986).
- [45] T. Asaka, S. Ejima and A. Watanabe, JHEP **1303** (2013) 125.
- [46] T. Asaka, S. Ejima and H. Ishida, JHEP **1104** (2011) 011.
- [47] A. D. Dolgov, S. H. Hansen, G. Raffelt and D. V. Semikoz, Nucl. Phys. B **580** (2000) 331.
- [48] A. D. Dolgov, S. H. Hansen, G. Raffelt and D. V. Semikoz, Nucl. Phys. B **590** (2000) 562.
- [49] L. Kawano, NASA STI/Recon Technical Report N **92**, 25163 (1992).
- [50] M. S. Smith, L. H. Kawano and R. A. Malaney, Astrophys. J. Suppl. **85**, 219 (1993).
- [51] S. Sarkar, Rept. Prog. Phys. **59**, 1493 (1996).
- [52] R. H. Cyburt *et al.*, Astrophys. J. Suppl. Ser. **189**, 240 (2010).
- [53] A. P. Serebrov and A. K. Fomin, Phys. Rev. C **82**, 035501 (2010).
- [54] G. J. Mathews, T. Kajino and T. Shima, Phys. Rev. D **71**, 021302 (2005).
- [55] A. Serebrov, V. Varlamov, A. Kharitonov, A. Fomin, Y. .Pokotilovski, P. Geltenbort, J. Butterworth and I. Krasnoschekova *et al.*, Phys. Lett. B **605**, 72 (2005).
- [56] M. Kusakabe *et al.*, Phys. Rev. D **79**, 123513 (2009).
- [57] T. Shima *et al.*, Phys. Rev. C **72**, 044004 (2005).
- [58] T. Kii, T. Shima, Y. Nagai and T. Baba, Nucl. Instrum. Meth. A **552**, 329 (2005).
- [59] F. C. Jones, Phys. Rev. **167**, 1159 (1968).
- [60] E. S. Ginsberg and D. Zaborowski, Commun. ACM, **18**, 200 (1975).
- [61] R. J. Protheroe, T. Stanev and V. S. Berezhinsky, Phys. Rev. D **51**, 4134 (1995).
- [62] V. S. Berezhinskii, S. V. Bulanov, V. A. Dogiel, V. L. Ginzburg and V. S. Ptuskin 1990, Astrophysics of Cosmic Rays, ed. V. S. Verezhinskii and V. L. Ginzburg (New York: North-Holland).
- [63] M. Kusakabe, A. B. Balantekin, T. Kajino and Y. Pehlivan, Phys. Lett. B **718**, 704 (2013).
- [64] M. Pettini and R. Cooke, arXiv:1205.3785 [astro-ph.CO].
- [65] W. Hu and J. Silk, Phys. Rev. Lett. **70**, 2661 (1993).
- [66] M. Seiffert, D. J. Fixsen, A. Kogut *et al.*, Astrophys. J. **734**, 6 (2011).
- [67] D. J. Fixsen, E. S. Cheng, J. M. Gales, J. C. Mather, R. A. Shafer and E. L. Wright, Astrophys. J. **473**, 576 (1996).
- [68] J. L. Feng, A. Rajaraman and F. Takayama, Phys. Rev. D **68**, 063504 (2003).
- [69] T. Asaka, M. Laine and M. Shaposhnikov, JHEP **0701** (2007) 091 [hep-ph/0612182].
- [70] E. W. Kolb and M. S. Turner, The early universe, Addison-Wesley, 1990.
- [71] A. Kusenko, S. Pascoli and D. Semikoz, JHEP **0511** (2005) 028.
- [72] T. Asaka and A. Watanabe, JHEP **1207** (2012) 112 [arXiv:1202.0725 [hep-ph]].
- [73] J. Beringer *et al.* [Particle Data Group Collaboration], Phys. Rev. D **86**, 010001 (2012).
- [74] L. M. Johnson, D. W. McKay and T. Bolton, Phys. Rev. D **56**, 2970 (1997).
- [75] D. Gorbunov and M. Shaposhnikov, J. High Energy Phys. **10**, 15 (2007).
- [76] J. M. Blatt and V. F. Weisskopf, *Theoretical nuclear physics* (Dover, Mineola, NY, 1991).
- [77] T. Kajino, S. M. Austin and H. Toki, Astrophys. J. **319**, 531 (1987).
- [78] C. Angulo, M. Arnould, M. Rayet *et al.* Nucl. Phys. A **656**, 3 (1999).
- [79] As for Eq. (51) in Ref. [36], the minus sign in the denominator of the third term on the right hand side is different from that of Eq. (9) in Ref. [59]. We adopt the latter plus sign.
- [80] <http://arcade.gsfc.nasa.gov>.
- [81] We should take into account only the photon as a relativistic species in thermal and chemical contact with e^\pm and photon itself during the cosmic epoch after BBN. This is because light active neutrinos had been decoupled from thermal bath before the onset of BBN at $T \sim 1$ MeV. We note previous studies (*e.g.*, [30, 68]) are erroneous since the g_{*S} factor included the contribution from neutrinos. The right numerical value in the following Eq. (III.3) is then higher than the previous suggestion by a factor of $2/3.91=1.96$.
- [82] We derived this effective time [43] which is slightly different from $t_{\text{eff}} = [\Gamma(\beta)]^{1/\beta} \tau_N$ in Ref. [65].
- [83] We note that coefficients of Eq. (A9) in Ref. [74] are erroneous.
- [84] Eq. (A10) of Ref. [74] should be multiplied by $1/4$ after coefficients are corrected.